Measurement of the Born cross sections of $e^+e^- \to D_s^{*+}D_{sJ}^-$ at BESIII

Tianyu Qi

Fudan University

Outline

- Motivation
- Data and MC samples
- Event Selection
- Background Analysis
- Main Fit
- Systematic Uncertainties
- Summary

Motivation

- In recent years, many Y states with $J^{PC} = 1^{--}$ above the open charm threshold have been discovered.
- In $e^+e^- \to Y \to \pi^+\pi^- J/\psi$ and $\pi^+\pi^-\psi(2S)$, events in $\pi^+\pi^-$ mass spectra tend to accumulate at the $f_0(980)$ nominal mass, which has an $s\bar{s}$ component. So, it is natural to search for Y states in $D_s\bar{D}_s$ meson spectrum.
- Belle report the discovery of $Y(4660)$ in the spectrum of $D_s^+ D_{s1}(2536)^-$.
- BESIII has updated c.m.s. energy over 4.6 GeV. We can observe $D_s^{*+} D_{s0}^*(2317)^-$, $D_s^{*+} D_{s1}(2460)^-$, $D_s^{*+} D_{s1}(2536)^-$, and $D_s D_{sJ}$'s at BESIII.

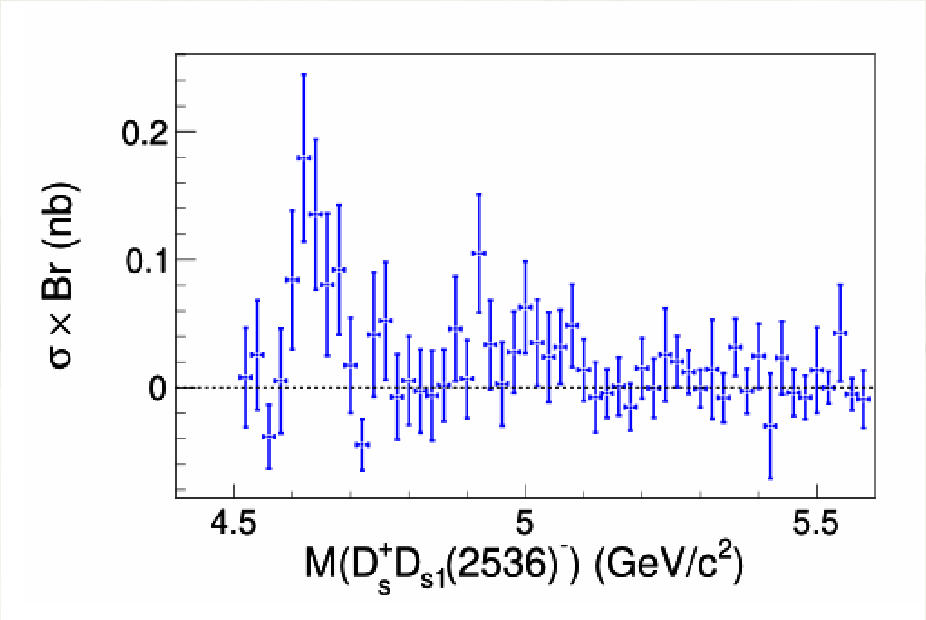

Belle, PRD 100, 111103 (2019)

Motivation

- Using data from 4.47 GeV to 4.6 GeV, BESIII measured the cross section of $e^+e^- \to D_s^+ D_{s1}(2460)^-$ and $D_s^{*+} D_{s1}(2460)^-$.
- Using data at 4.6 GeV, BESIII measured the cross section of $e^+e^- \to D_s^+ K^- \overline{D}^{(*)0}$, where $K^- \overline{D}^{(*)0}$ has a significant contribution from $D_{s1}(2536)^-$ and $D_{s2}^*(2573)^-$.

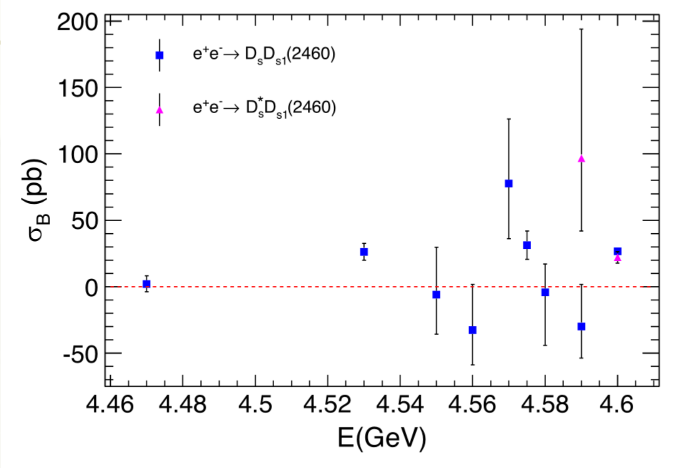

PRD 101, 112008 (2020)

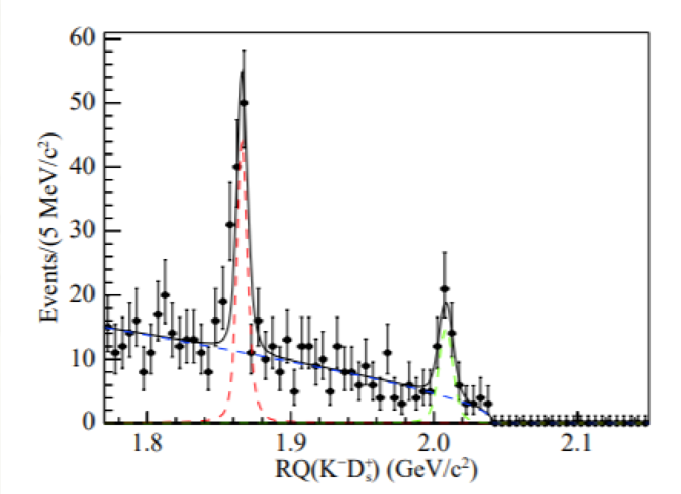

CPC Vol. 43, No. 3 031001 (2019)

Data and MC samples

- Data samples from 4.6 GeV to 4.7 GeV are used.
- To determine detector efficiency and optimize event selection, we generated MC samples of $e^+e^- \to D_s^{*+}D_{sJ}^-$, where D_{sJ}^- includes $D_{s0}^*(2317)^-$, $D_{s1}(2460)^-$, and $D_{s1}(2536)^-$ ($D_{s1}(2536)^-$ only at $\sqrt{s} \geq 4.66$ GeV), with $D_s^{*+} \to \gamma D_s^+$ and $D_s^+ \to K^+K^-\pi^+$. The D_{sJ}^- decays to all possible final states.
- Inclusive MC samples at 4.6 GeV and 4.68 GeV are used to check all possible backgrounds, which includes open charm and hadron processes.

$\sqrt{s}$ (MeV)	Luminosity (pb^{-1})
4600	586.9 ± 3.9
4612	102.50 ± 0.29
4626	511.06 ± 1.45
4640	541.37 ± 1.54
4660	523.63 ± 1.49
4680	1643.38 ± 4.66
4700	526.20 ± 1.49

(2013, 2020)

Event Selection

- We reconstruct a D_s^+ using $K^+K^-\pi^+$, and reconstruct a D_s^{*+} using γD_s^+. Then we search for D_{sJ}^- in D_s^{*+} recoil mass spectrum.
- Charge conjugate mode is implied.
- Charged track selection:
  - Closest approach to the beam axis $V_{xy} < 1$ cm, $V_z < 10$ cm;
  - Polar angle $|\cos\theta| < 0.93$.
- Particle ID
  - Kaon: $\mathrm{Prob}(K) > \mathrm{Prob}(\pi)$ and $\mathrm{Prob}(K) > 0.001$;
  - Pion: $\mathrm{Prob}(\pi) > \mathrm{Prob}(K)$ and $\mathrm{Prob}(\pi) > 0.001$.
- Require at least three good charged tracks and one good photon.
- All combinations of $K^+K^-\pi^+$ which passed a vertex fit is kept.

Event Selection

- In addition to BESIII common tracking and PID selection criteria, we perform a mass-constraint 2C kinematic fit to $D_s^+ \to K^+K^-\pi^+$ and $D_s^{*+} \to \gamma D_s^+$ candidate, and require $\chi^2_{2C} < 10$ to suppress background.
- We use $D_s^+ \to \phi(\to K^+K^-)\pi^+$ and $D_s^+ \to \overline{K}^{*0}(\to K^-\pi^+)\pi^-$ sub-modes to improve the ratio of signal over background. We require $\left|M(K^+K^-) - m_\phi\right| < 9\ \mathrm{MeV}/c^2$ for $\phi\pi$ mode and $|M(K^-\pi^+) - m_{\overline{K}^{*0}}| < 84\ \mathrm{MeV}/c^2$ for $K\pi$ mode ($\sim 3\sigma$).

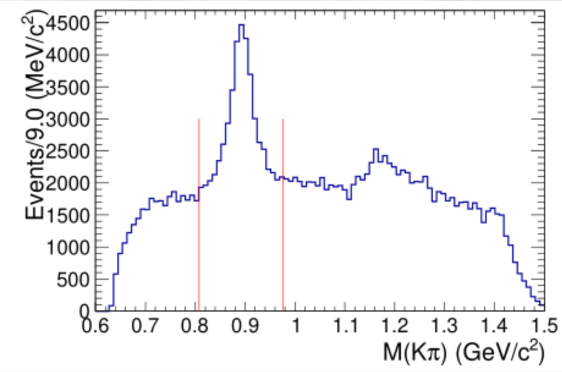

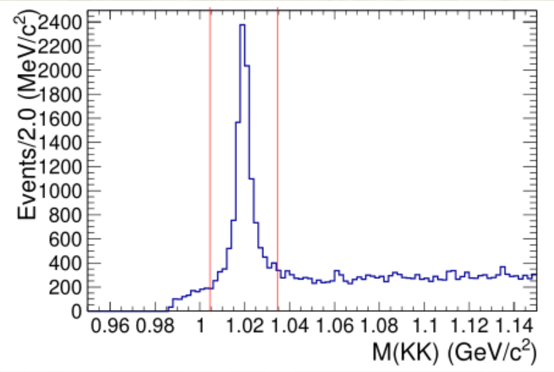

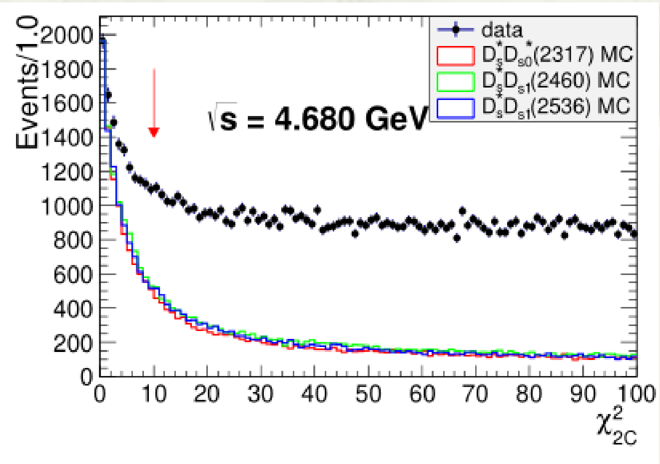

Figures from 4.68 GeV data are shown as examples.

Event Selection

- The $\chi^2_{2C} < 10$ criteria is optimized using FOM value.
- $\text{FOM} = \frac{s}{\sqrt{s+B}}$, where s stands for the expected number of observed signal yields, computed using signal MC samples, and B stands for the background event count from inclusive MC samples in the signal range.

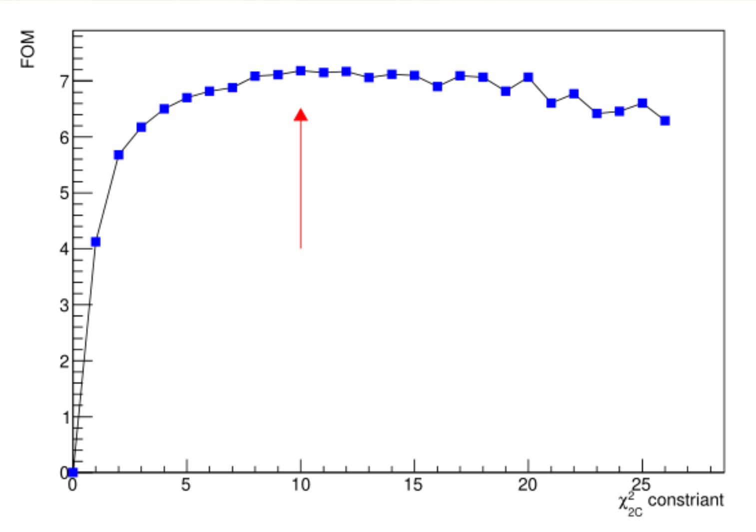

Background Analysis

- We used the MC truth matching to check for combinatorial background from wrong combination. The distribution of D_s^{*+} recoil mass from these events is smooth.

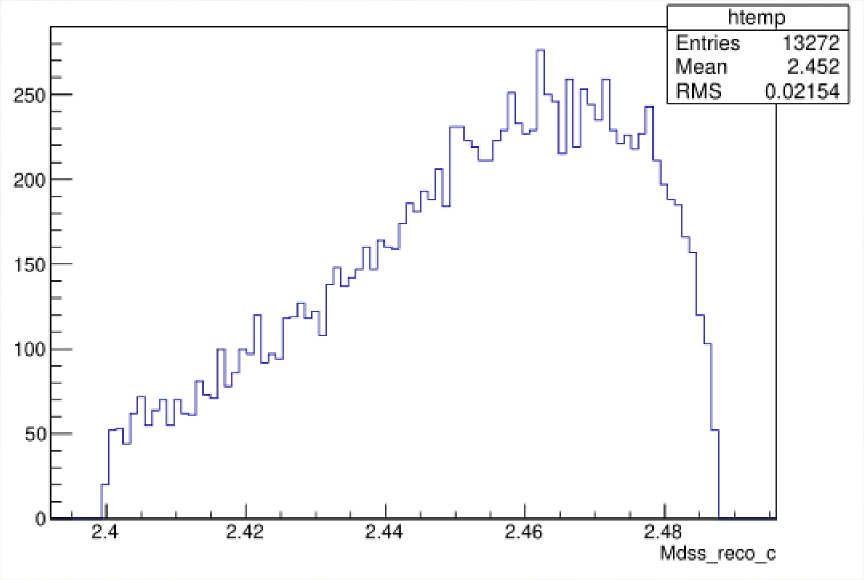

Background analysis

- For the background analysis, inclusive MC samples of open charm processes are used, where no $e^+e^- \to D_s^{*+}D_{sJ}^-$ events are generated.
- The $M^{\rm rec}_{D_s^{*+}}$ distributions from inclusive MC samples are shown below, where $M^{\rm rec}_{D_s^{*+}} = RM(\gamma K^+K^-\pi^+) + M(\gamma K^+K^-\pi^+) - m_{D_s^{*+}}$, in order to improve the D_s^{*+} resolution.
- A maximum likelihood fit is performed to the $M^{\rm rec}_{D_s^{*+}}$ distribution, where an Argus function is used for background, and MC-derived signal shapes are used. The fitted signal yields are consistent with zero.

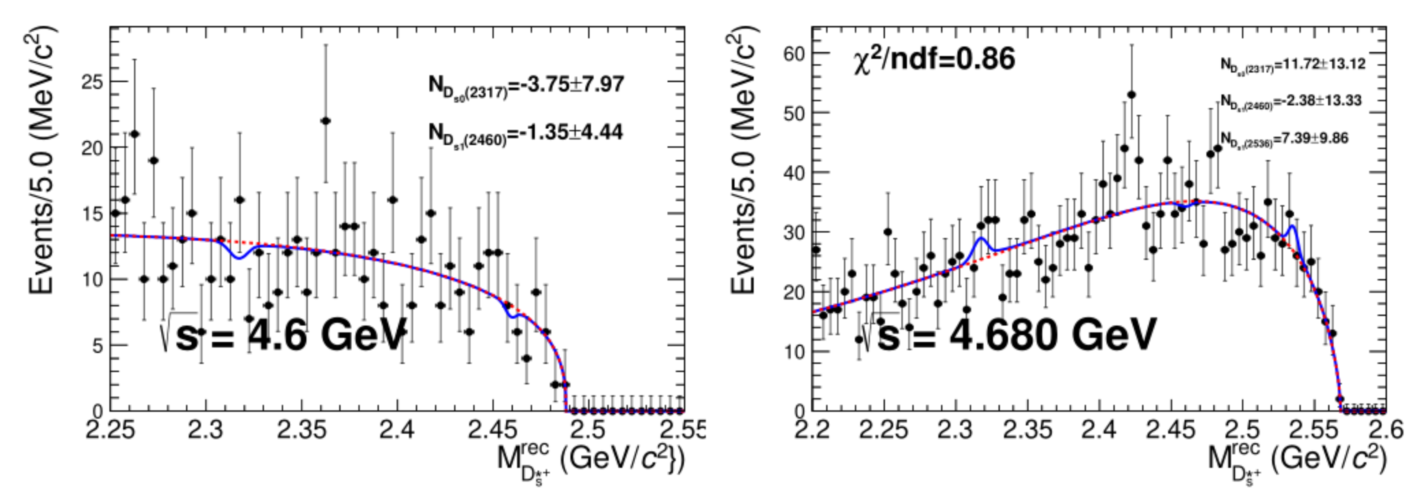

Main Fit

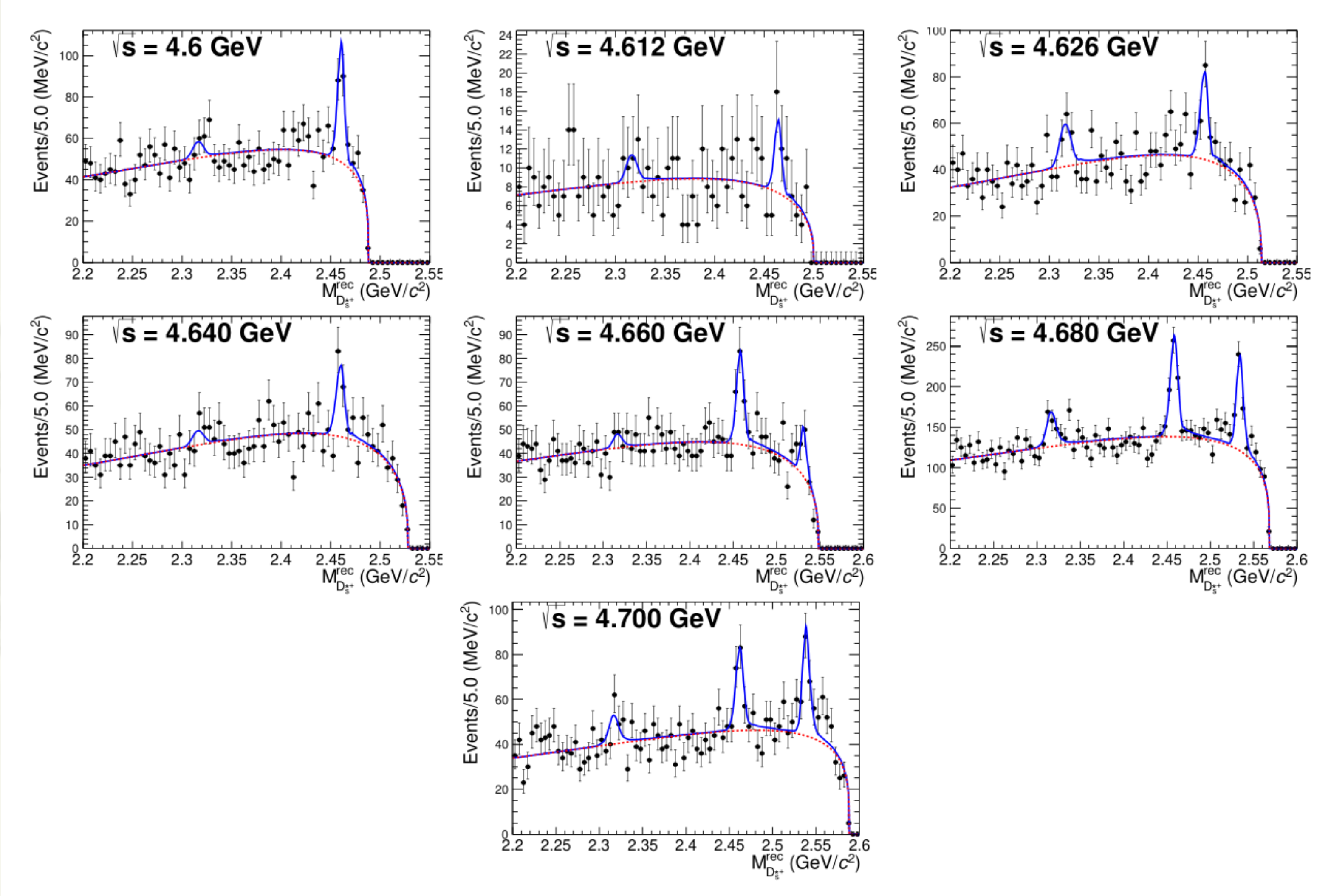

√s = 4.6 GeV
√s = 4.612 GeV
√s = 4.626 GeV
√s = 4.640 GeV
√s = 4.660 GeV
√s = 4.680 GeV
√s = 4.700 GeV
Events/5.0 (MeV/c²)
M^rec_{D_s^{*+}} (GeV/c²)

Main Fit

$\sqrt{s}$ (GeV)	$D_s^* D_{s0}^*(2317)^-$		$D_s^* D_{s1}(2460)^-$		$D_s^* D_{s1}(2536)^-$	
	significance	σ_B (pb) ($\sigma_{U.L.}$)	significance	σ_B (pb) ($\sigma_{U.L.}$)	significance	σ_B (pb) ($\sigma_{U.L.}$)
4.6	1.4σ	$6.8^{+5.0}_{-4.8}$ (14.8)	7.1σ	$31.2 \pm 5.2 \pm 3.7$	-	-
4.612	1.2σ	$14.7^{+13.3}_{-12.0}$ (34.7)	2.5σ	$26.1^{+12.8}_{-11.5}$ (44.4)	-	-
4.626	3.6σ	$19.3 \pm 5.8 \pm 2.0$	5.6σ	$29.1 \pm 6.0 \pm 2.6$	-	-
4.64	1.2σ	$6.0^{+5.2}_{-5.0}$ (14.1)	4.7σ	$22.8 \pm 5.6 \pm 2.3$	-	-
4.66	1.2σ	$5.8^{+5.3}_{-5.0}$ (14.1)	6.1σ	$31.1 \pm 6.0 \pm 2.7$	3.4σ	$13.4 \pm 4.4 \pm 1.7$
4.68	4.9σ	$13.9 \pm 3.0 \pm 1.4$	11.0σ	$31.9 \pm 3.3 \pm 2.5$	10.1σ	$26.9 \pm 3.1 \pm 2.3$
4.7	2.7σ	$13.7^{+5.6}_{-5.4}$ (21.4)	5.8σ	$30.8 \pm 6.0 \pm 2.6$	7.0σ	$35.1 \pm 6.0 \pm 3.0$

The first uncertainties are statistical and the second are systematic.
For the 90% C.L. upper limit, systematic uncertainties are included.

$$\sigma_B(e^+e^- \to D_s^{*+} D_{sJ}^-) = \frac{N_{\rm fit}}{\mathscr{L}_{\rm int}(1+\delta)(1+\delta^{\rm vp})\varepsilon_{D_s^{*+}}\mathscr{B}(D_s^{*+} \to \gamma D_s^+)\mathscr{B}(D_s^+ \to K^+K^-\pi^+)}$$

Main Fit

- The 90% upper limits are obtained using the likelihood curve:

$$\int_0^{N_{\mathrm{U.L.}}} \mathcal{L}(x)dx = 0.9 \int_0^{\infty} \mathcal{L}(x)dx\,,$$

- where x stands for the assumed yield of D_{sJ}^{-} signal and $\mathcal{L}(x)$ is the maximum likelihood of the fit.

Systematic Uncertainties

- The systematic uncertainties are divided into two categories: multiplicative and additive.
- Multiplicative uncertainties include:
  - PID and tracking;
  - Photon detection;
  - Statistic uncertainties of efficiencies;
  - Kinematic fit;
  - ISR factor;
  - Vacuum polarization factor;
  - Luminosity;
  - Intermediate branching fraction.
- Additive uncertainties (Fit related) include:
  - D_{sJ}^{-} mass;
  - Fit range;
  - Background shape.

Systematic Uncertainties

- For energy points with signal significance $< 3\sigma$, the systematic uncertainties are taken into account in two steps.
- First, we keep the most conservative upper limit among the additive systematic uncertainties.
- Next, we convolve the likelihood curve with a Gaussian function representing the total multiplicative systematic uncertainties.

Summary

- We observed $e^+e^- \to D_s^{*+}D_{s0}^*(2317)^-$, $D_s^{*+}D_{s1}(2460)^-$, and $D_s^{*+}D_{s1}(2536)^-$ above 4.6 GeV, and the Born cross sections are measured. Upper limits where the signal significance $< 3\sigma$ are given. The error bars in the plot below only includes statistical errors.
- The uncertainties are large, and no significant structures are observed.
- Current: PubComm step, intended for PRD.
- The analysis of $D_s^+ D_{sJ}^-$ is ongoing.

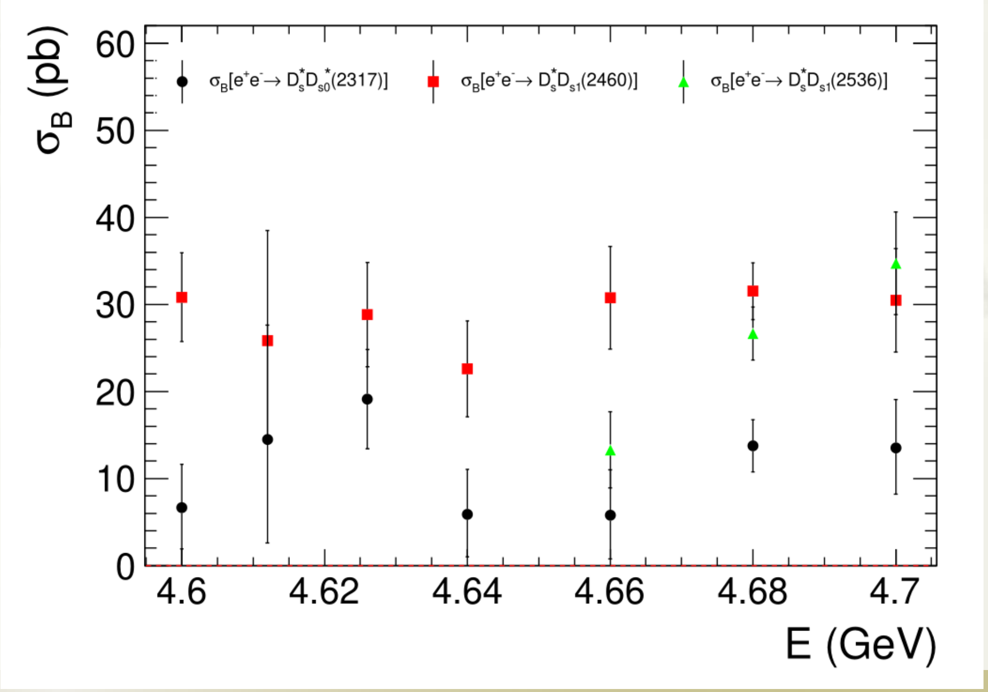

Thanks for listening!

Backup

Topo analysis

rowNo	decay tree	nEtrs
1	$e^+e^- \to D_s^- D_s^{*+}, D_s^- \to \pi^- K^+ K^-, D_s^{*+} \to D_s^+ \gamma, D_s^+ \to \pi^+ K^+ K^-$	8
2	$e^+e^- \to D_s^{*+} D_s^{*-}, D_s^{*+} \to D_s^+ \gamma, D_s^{*-} \to D_s^- \gamma, D_s^+ \to \rho^+ \phi, D_s^- \to \pi^- K^+ K^-,$ $\rho^+ \to \pi^0 \pi^+, \phi \to K^+ K^-$	6
3	$e^+e^- \to b_1^+ K_1^{\prime 0} \bar{K}_1^{\prime -}, b_1^+ \to \pi^+ \omega, K_1^{\prime 0} \to \pi^0 K^*, \bar{K}_1^{\prime -} \to \pi^- \bar{K}^*, \omega \to \pi^0 \pi^+ \pi^-,$ $K^* \to \pi^- K^+, \bar{K}^* \to \pi^+ K^-$	6
4	$e^+e^- \to D_s^{*+} D_s^{*-}, D_s^{*+} \to D_s^+ \gamma, D_s^{*-} \to D_s^- \gamma, D_s^+ \to \pi^+ K^+ K^-, D_s^- \to \rho^- \eta,$ $\rho^- \to \pi^0 \pi^-, \eta \to \pi^0 \pi^0 \pi^0$	5
5	$e^+e^- \to D_s^{*+} D_s^{*-}, D_s^{*+} \to D_s^+ \gamma, D_s^{*-} \to D_s^- \gamma, D_s^+ \to \rho^+ \eta, D_s^- \to \pi^- K^+ K^-,$ $\rho^+ \to \pi^0 \pi^+, \eta \to \pi^0 \pi^+ \pi^-$	5
6	$e^+e^- \to D_s^{*+} D_s^{*-}, D_s^{*+} \to D_s^+ \gamma, D_s^{*-} \to D_s^- \gamma, D_s^+ \to \bar{K}^* K^{*+}, D_s^- \to \pi^- K^+ K^-,$ $\bar{K}^* \to \pi^+ K^-, K^{*+} \to \pi^0 K^+$	4
7	$e^+e^- \to b_1^0 K_1^{\prime +} \bar{K}_1^{\prime -}, b_1^0 \to \pi^0 \omega, K_1^{\prime +} \to \pi^+ K^*, \bar{K}_1^{\prime -} \to \pi^- \bar{K}^*, \omega \to \pi^0 \pi^+ \pi^-,$ $K^* \to \pi^- K^+, \bar{K}^* \to \pi^+ K^-$	4
8	$e^+e^- \to b_1^- \bar{K}_1^{\prime 0} K_1^{\prime +}, b_1^- \to \pi^- \omega, \bar{K}_1^{\prime 0} \to \pi^0 \bar{K}^*, K_1^{\prime +} \to \pi^+ K^*, \omega \to \pi^0 \pi^+ \pi^-,$ $\bar{K}^* \to \pi^+ K^-, K^* \to \pi^- K^+$	4
9	$e^+e^- \to b_1^+ K_1^{\prime 0} \bar{K}_1^{\prime -}, b_1^+ \to \pi^+ \omega, K_1^{\prime 0} \to \pi^- K^{*+}, \bar{K}_1^{\prime -} \to \pi^- \bar{K}^*, \omega \to \pi^0 \pi^+ \pi^-,$ $K^{*+} \to \pi^0 K^+, \bar{K}^* \to \pi^+ K^-$	4
10	$e^+e^- \to D_s^+ D_s^{*-}, D_s^+ \to \pi^+ K^+ K^-, D_s^{*-} \to D_s^- \gamma, D_s^- \to \pi^- K^+ K^-$	4
11	$e^+e^- \to D_s^{*+} D_s^{*-}, D_s^{*+} \to D_s^+ \gamma, D_s^{*-} \to D_s^- \gamma, D_s^+ \to \pi^+ K^+ K^-, D_s^- \to \rho^- \phi,$ $\rho^- \to \pi^0 \pi^-, \phi \to K^+ K^-$	4
12	$e^+e^- \to D_s^{*+} D_s^{*-}, D_s^{*+} \to D_s^+ \gamma, D_s^{*-} \to D_s^- \gamma, D_s^+ \to \pi^+ K^+ K^-, D_s^- \to \rho^- \eta',$ $\rho^- \to \pi^0 \pi^-, \eta' \to \pi^+ \pi^- \gamma^F$	4

Combined data sample

- 6.9σ, 11.3σ, 6.3σ